


Reducing the Energy Storage Requirements of Modular Multilevel Converters with Optimal Capacitor Voltage Trajectory Shaping

Conference Paper**Author(s):**

Fuchs, Simon; Jeong, Min; Biela, Jürgen 

Publication date:

2020

Permanent link:

<https://doi.org/10.3929/ethz-b-000495889>

Rights / license:

In Copyright - Non-Commercial Use Permitted

Originally published in:

<https://doi.org/10.23919/EPE20ECCEurope43536.2020.9215757>

Reducing the Energy Storage Requirements of Modular Multilevel Converters with Optimal Capacitor Voltage Trajectory Shaping

Simon Fuchs, Min Jeong, Jürgen Biela
 Laboratory for High Power Electronic Systems (HPE)
 Email: fuchssim@ethz.ch, jbiela@ethz.ch
 ETH Zürich, Switzerland

Keywords

«HVDC», «Optimal control», «High power density systems», «High voltage power converters», «Harmonics»

Abstract

The required module capacitance value is a driving factor of the volume and cost of modular multilevel converters (MMC). In order to minimize the required capacitance value, an optimal circulating current and common mode (CM) voltage injection strategy which keeps the conduction losses and die CM voltage as low as possible is proposed in this paper. Unlike previous methods from literature that only focus on minimizing the amplitude of energy fluctuation in the arm capacitors, the proposed optimization procedure is based on the optimal shaping of both the arm voltages and energies. As a result, the proposed optimization scheme achieves a further reduction in the required capacitance value of up to 42 % compared to existing methods. The procedure is validated with closed loop simulation results covering the full operating range of an exemplary MMC.

1 Introduction

The Modular Multilevel Converter (MMC, [1]) represents one of the standard topologies for converters operating at medium to high voltages [2, 3]. However, a major drawback of the MMC is its relatively high energy storage requirements resulting in large module capacitors that significantly contribute to the MMC's volume, weight, and cost.

The large module capacitors are required because of the single phase characteristics of the six MMC arms (cf. Fig. 1). In each arm, the instantaneous AC and DC power are not equal, which causes a fluctuation in the energy stored in the module capacitors. This leads to a fluctuation/ripple in the module capacitor voltages and therefore also in the available arm voltage v^Σ (sum of all capacitor voltages) as shown in Fig. 2a. The smaller the module capacitance value, the higher the amplitude of this voltage fluctuation. In [4], the minimum required capacitance value for the standard operation of an MMC is derived: The available arm voltage v_{1u}^Σ is always higher or just equal to the required arm output voltage v_{1u} and always less or just equal to the maximum allowed available arm voltage ($N \cdot V_{C,\max}$) as shown in Fig. 2b.

In order to decrease the amplitude of the arm energy/capacitor voltage fluctuation, many examples that inject circulating currents are proposed in literature. The amplitude and phase of the injected harmonics are either

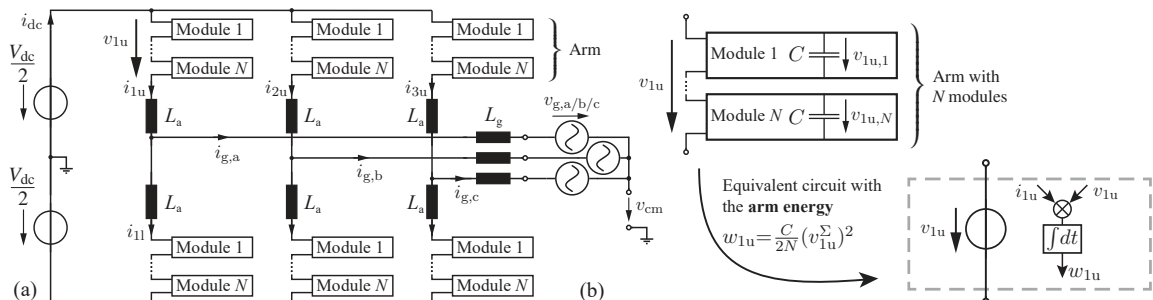


Fig. 1: (a) Three phase MMC. N modules form one out of six arms. (b) One arm can be represented with an energy storage, that integrates the arm power $w_{1u} = i_{1u} \cdot v_{1u}$. The indices represent the upper arm of the first phase.

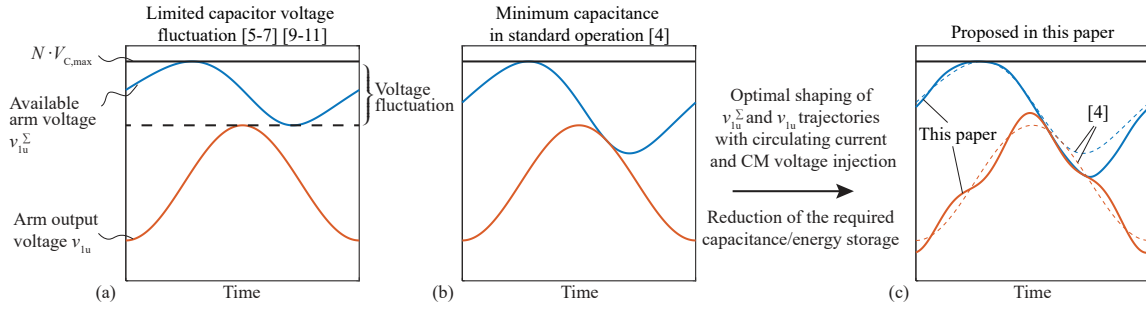


Fig. 2: Different (available) arm voltage trajectories for active power transfer: (a) For MMC design with limited capacitor voltage ripple, (b) minimum required capacitance/energy storage with standard operation (no circulating currents, no CM voltage injection) as shown in [4], (c) Optimal shaping of the available arm voltage (v_{1u}^{Σ}) and arm output voltage (v_{1u}) by circulating current and common mode (CM) voltage injection. The indices represent the upper arm of the first phase.

determined analytically [5, 6, 7] or using offline optimizations [8, 9, 10]. In some cases, the circulating current injection is also combined with additional harmonics in the CM voltage v_{cm} at the grid side of the MMC [11]. If there is no star-point connection at the grid side (see Fig. 1a), this has no influence on the grid currents but decreases the maximum required arm output voltage [4, 12].

The reduced energy fluctuation in the MMC arms can be used to reduce the required module capacitance value because the same voltage fluctuation can be achieved with a lower capacitance value. However, reducing only the arm energy fluctuation does not necessarily minimize the required capacitance value because it does not consider the relation between the trajectories of the required arm output voltage and the available arm voltage as described in [4]. All listed references aim to decrease the fluctuation of the capacitor voltage/energy and do not consider the actually required capacitance value or the trajectories of the arm output voltage and the available arm voltage. An exception is the procedure described in [8], which aligns the peak of the available arm voltage with the peak of the required arm output voltage by using a second harmonic circulating current. The analysis is however limited to a second harmonic in the circulating current.

To complete the analysis and further reduce the required capacitance value, this paper proposes an optimization procedure that identifies the optimal trade-off between the reduction in the required capacitance, the (semiconductor conduction) losses, and the CM voltage amplitude. The optimization procedure searches for optimal combinations of the second and fourth harmonics in the circulating current as well as the third and ninth harmonic in the CM voltage. The required capacitance value is determined with an extended version of the procedure presented in [4], in order to consider the actual trajectories of the available arm voltage and the arm output voltage (Fig. 2c). As a result, a three-dimensional Pareto front/surface is calculated, which allows to analyse the influence of combining a CM voltage and a circulating current injection on the reduction of the required capacitance. Variable output frequencies as required in drive applications are not explicitly considered.

The paper is organized as follows: In section 2, all important modelling equations required to determine the steady state trajectories of the MMC are reviewed. The proposed optimization scheme is presented in section 3. In section 4, the optimization results for an exemplary MMC parameter set are shown, analysed, and compared to some benchmark schemes given in literature. Section 5 presents simulation results and proposes a possible controller implementation to realize the harmonics injection within a closed loop control system.

2 Steady State Trajectories of the MMC

In the following, analytical expressions for the steady state trajectories of the MMC as shown in Fig. 1 are introduced. For the sake of simplicity, the analysis is limited to transferring purely active power P only. The expressions are given for the upper arm of the first phase (index '1u').

Arm Currents

As introduced e.g. in [4], the arm currents consist of a DC component $i_{1u,dc}$ and an AC component $i_{1u,ac}$ that has the same frequency as the grid. These two components are necessary for the operation of the MMC because they exchange the power with the DC side and AC side respectively. They can be expressed as

$$i_{1u,dc} = \frac{i_{dc}}{3} = \frac{P}{3 \cdot V_{dc}}, \quad i_{1u,ac} = \frac{i_g}{2} \cdot \cos(\omega t) = \frac{P}{2\sqrt{3} \cdot V_g} \cdot \cos(\omega t). \quad (1)$$

In this paper, a second and fourth harmonic circulating current are added as suggested in [9]. Note, that only even harmonics that are not divisible by three are allowed for circulating currents, because all other harmonics have an

effect on either the DC or the AC side currents. With the circulating current harmonics, the total arm current is

$$i_{1u} = i_{1u,dc} + i_{1u,ac} + \hat{i}_{c2} \cdot \cos(2\omega t + \varphi_{c2}) + \hat{i}_{c4} \cdot \cos(4\omega t + \varphi_{c4}), \quad (2)$$

where \hat{i}_{c2} as well as \hat{i}_{c4} are the amplitudes and φ_{c2} as well as φ_{c4} are the phase angles of the circulating current harmonics.

Arm Output Voltages

To simplify the analysis, the MMC arms are regarded as continuously controllable voltage sources [13]. Therefore, the arm output voltage is composed of a DC and an AC component given as

$$v_{1u,dc} = \frac{V_{dc}}{2}, \quad v_{1u,ac} = \sqrt{\frac{2}{3}} \cdot V_g \cdot \cos(\omega t). \quad (3)$$

In this paper, a third and a ninth harmonic Common Mode (CM) voltage are added to the AC component. CM harmonics divisible by three do not drive a current on the DC side nor on the AC side, if the AC side star point is not grounded. However, the 6th harmonic is omitted because even CM harmonics lead to a non-symmetric energy fluctuation in the upper and lower MMC arms, which is not desirable within the presented optimization routine, because one would have to consider the upper and lower arms separately. With the CM voltage harmonics, the total arm voltage is given as

$$v_{1u} = v_{1u,dc} - v_{1u,ac} - \hat{v}_{cm3} \cdot \cos(3\omega t + \varphi_{cm3}) - \hat{v}_{cm9} \cdot \cos(9\omega t + \varphi_{cm9}), \quad (4)$$

where \hat{v}_{cm3} as well as \hat{v}_{cm9} are the amplitudes and φ_{cm3} as well as φ_{cm9} are the phase angles of the CM voltage harmonics. The voltages necessary to drive the arm currents through the arm inductors and resistors are neglected here, as they are typically very small compared to the other parts of the arm output voltage. However, the procedure presented in this paper does not change in case this voltage drop is included.

Arm Energy and Available Arm Voltage

The available arm voltage v_{1u}^Σ can be expressed with the energy w_{1u} stored in all capacitors of the arm. As depicted in Fig. 1(b) his energy can be derived with the arm power p_{1u} given as

$$w_{1u}(t) = \int_0^t p_{1u}(\tau) d\tau + w_{dc}, \quad \text{with} \quad p_{1u} = v_{1u} \cdot i_{1u}, \quad (5)$$

where $w_{dc} = C/N \cdot (v_{dc}^\Sigma)^2/2$ is the average arm energy during a grid period defined by the DC offset v_{dc}^Σ of the available arm voltage. It will be shown in the first part of section 3 how the optimal average arm energy/DC offset voltage is determined. Inserting (1), (2), (3) and (4) into (5) results in a long expression that is omitted here for space reasons.

3 Optimization Procedure

Based on the equations presented in section 2, an optimization procedure determining the optimal harmonics injection is presented in the following. First, the determination of the minimum capacitance value is described based on fixed trajectories with given circulating currents and CM voltages. Then, the trajectory shaping optimization procedure is explained to find the optimal combination(s) of circulating current and CM voltage harmonics injection.

Minimum Capacitance Determination

[4] provides a procedure to determine the minimum module capacitor value for a given set of MMC ratings (AC/DC voltage, power, number of modules, maximum module voltage) when no harmonics in the arm currents/CM voltage are assumed. In the following, the relations derived in [4] are shortly revised and adopted to be used with given harmonics in the arm currents/CM voltage.

There are two important factors k_{max} (relation between the max. allowed available arm voltage and the DC voltage) and k_{dc} (relation between the DC offset voltage v_{dc}^Σ and the DC voltage) given as

$$k_{max} = \frac{N \cdot V_{C,max}}{V_{dc}}, \quad k_{dc} = \frac{v_{dc}^\Sigma}{V_{dc}}, \quad (6)$$

where $V_{C,\max}$ is the maximum allowed capacitor voltage of the MMC's modules. It can be shown (cf. [4]) that the minimum k_{dc} fulfilling

$$k_{dc} \geq \sqrt{\frac{\frac{v_{1u}^2(t)}{V_{dc}^2} - k_{\max}^2 \cdot \frac{w_{1u}(t) - w_{dc}}{w_{1u,\max} - w_{dc}}}{1 - \frac{w_{1u}(t) - w_{dc}}{w_{1u,\max} - w_{dc}}}}, \quad \forall t \in \left[0, \frac{2\pi}{\omega}\right] \quad \text{with} \quad w_{1u,\max} = \max_{t \in \left[0, \frac{2\pi}{\omega}\right]} w_{1u}(t) \quad (7)$$

for the complete grid period yields the minimum required module capacitance

$$C_{\min} = \frac{2N}{V_{dc}^2} \cdot \frac{w_{1u,\max} - w_{dc}}{k_{\max}^2 - k_{dc}^2}. \quad (8)$$

If no harmonics in the circulating current and the CM voltage are injected, the trajectories given in Fig. 2b result, where the available arm voltage is always just bigger or equal to the required arm voltage and always just smaller or equal to $N \cdot V_{C,\max}$.

Note that w_{dc} does not have to be known to solve this. The difference $w_{1u} - w_{dc}$ is just used to express the integral part of (5). Therefore, w_{dc} and v_{dc}^Σ are rather the second result of the capacitance value minimization, because they are given with the chosen k_{dc} as

$$v_{dc}^\Sigma = k_{dc} \cdot \frac{V_{dc}}{N} \quad \text{and} \quad w_{dc} = N \cdot C \cdot \frac{(v_{dc}^\Sigma)^2}{2}. \quad (9)$$

Optimal Trajectory Shaping

The vector of optimization variables \mathbf{x} contains the amplitude and phase angles of the 2nd and 4th harmonics in the circulating currents as well as the 3rd and 9th harmonics in the CM voltage, such that

$$\mathbf{x} = [\hat{i}_{c2} \quad \varphi_{c2} \quad \hat{i}_{c4} \quad \varphi_{c4} \quad \hat{v}_{cm3} \quad \varphi_{cm3} \quad \hat{v}_{cm9} \quad \varphi_{cm9}]. \quad (10)$$

Modifying the shape of the energy/available arm voltage trajectory comes at a cost of a CM voltage at the MMC's AC side and/or changed losses in the MMC's semiconductors. There is no general optimally shaped trajectory but rather a Pareto front representing the optimal trade-off between required module capacitance value, semiconductor losses and CM voltage amplitude. Therefore, three fitness functions are used to perform a multi-objective optimization:

1. The reduction in the required capacitance value for circulating current and CM voltage harmonics given in \mathbf{x} can be stated as

$$J_{\text{cap}} = C_{\min}(\mathbf{x}) / C_{\min}(\mathbf{x} = \mathbf{0}). \quad (11)$$

The value of the required capacitance is determined by the procedure described in the previous subsection 'Minimum Capacitance Determination' (7) - (9).

2. By injecting circulating current harmonics, the arm currents that cause losses in the semiconductors and arm inductors are changed. Here, the change in the arm current mean rectified value is considered. Using (1) and (2), this change can be expressed with

$$J_{\text{current}} = I_{\text{av,rect}}(\mathbf{x}) / I_{\text{av,rect}}(\mathbf{x} = \mathbf{0}), \quad \text{where} \quad I_{\text{av,rect}}(\mathbf{x}) = \frac{\omega}{2\pi} \int_{t=0}^{\omega/2\pi} |i_{1u}(t, \mathbf{x})| dt. \quad (12)$$

This fitness function can also be replaced by the increase in the RMS value of the arm current or any combination J_{loss} of RMS and mean rectified current to represent the increase of semiconductor and arm inductor losses due to the injected circulating currents ($J_{\text{loss}} = a \cdot I_{\text{av,rect}}(\mathbf{x}) + b \cdot I_{\text{RMS}}(\mathbf{x})$, where a and b depend on the candidate semiconductor switches and the specific inductor implementation). This does not cause any major change in the proposed algorithm.

3. The third important parameter is the maximum amplitude of the CM voltage. This is the voltage of the star-point of a transformer which defines the isolation requirements of the grid transformer as denoted in Fig. 1a. Therefore,

$$J_{\text{CM}} = \max_{t \in [0, 2\pi/\omega]} |\hat{v}_{cm3} \cdot \cos(3\omega t + \varphi_{cm3}) + \hat{v}_{cm9} \cdot \cos(9\omega t + \varphi_{cm9})| \quad (13)$$

can be used to formulate the cost associated with the injected common mode voltage harmonics.

There are also constraints that must be considered:

1. All entries of \mathbf{x} must be greater than zero and the phase angles are constrained to the interval $[0 \dots 2\pi]$.
2. In order to consider also the maximum current capabilities of the used semiconductors and/or the saturation current of the used inductors, the arm currents must be constraint to a maximum absolute value i_{\max} , such that

$$|i_{1u}(t, \mathbf{x})| \leq i_{\max} \quad \forall t \in [0, 2\pi/\omega]. \quad (14)$$

3. In case of half-bridge based MMC modules, the arm output voltage has to be constrained to be greater than zero. This results in

$$v_{1u,dc} - v_{1u,ac} - \hat{v}_{cm3} \cdot \cos(3\omega t + \varphi_{cm3}) - \hat{v}_{cm9} \cdot \cos(9\omega t + \varphi_{cm9}) \geq 0 \quad \forall t \in [0, 2\pi/\omega]. \quad (15)$$

In case of full-bridge MMC modules this constraint is not needed.

To perform a multi-criteria optimization, one could use a brute force approach, but with \mathbf{x} having eight entries this takes a very long time if accurate results should be achieved. Therefore, the genetic algorithm [14] contained in the Matlab Global Optimization Toolbox is used to generate the results presented in the next section.

4 Optimization Results and Discussion

In this section the results of the optimization procedure described in section 3 for the exemplary MMC parameters given in Table I (MV case, see Fig. 3) and Table II (HVDC case, see Fig. 5) are presented and discussed. The resulting three-dimensional Pareto front is shown in part (c) of both figures. Part (a), (b), and (d) represent the top and side view of this Pareto front. Every black dot represents a Pareto optimal optimization result, which means, that it is better in two out of three of the considered cost functions than all other solutions. There are also solid lines with three different colours drawn within the Pareto fronts:

- The red lines — represent the Pareto front, when the CM voltage amplitude is not restricted. In part (c), one of the red lines is the projection of the other red line onto the xy -plane. If the CM voltage amplitude is not considered, the points on the red line provide the best trade-off between capacitance value reduction and arm current increase with the given maximum arm current. Note that the red line also represents the maximum meaningful CM voltage that helps to reduce the required capacitance value. Higher values would not result in a lower required capacitance value as shown in part (d) of the figures.
- The green lines — represent the Pareto front if no CM voltage injection is allowed.
- The blue lines — represent the Pareto front, when the CM voltage amplitude is limited to $\hat{V}_g/6$.

There is a point marked with a green star $*$ in both figures. This point features the combination of CM voltage and circulating harmonic injection that results in the lowest possible required capacitance value with the given parameters and maximum arm current. Besides this, there is also a point marked with a pink star $*$ representing the lowest possible required capacitance value when avoiding CM voltage injection. The time domain trajectories of the voltages and currents of the upper arm of the first phase for these design points are shown in Fig. 4 for one grid period using exactly the minimum required capacitance value.

Comparison with Existing Methods

Fig. 3 and 5 also contain the results for different methods given in the literature, if the fitness functions proposed in this paper are applied to the given circulating current and CM voltage trajectories proposed in the respective publication. It can be seen that the optimization proposed in this paper leads to a lower required capacitance value with a lower mean rectified current in any case. Furthermore, the CM voltage injection proposed in the literature references does always lead to an increase in the required capacitance value (compare [5] with and without CM as well as [7] Methods B and C in Fig. 3c).

The procedure presented in [9, 10, 11] minimizes the energy fluctuation Δw_{1u} in the module capacitors given by

$$\Delta w_{1u} = \max_{t \in [0, \frac{2\pi}{\omega}]} w_{1u}(t) - \min_{t \in [0, \frac{2\pi}{\omega}]} w_{1u}(t). \quad (16)$$

Table I: MMC PARAMETERS (MV CASE)

Symbol		Value	Symbol		Value
V_g	Rated grid voltage	9kV	I_g	Rated grid current	22.681 A
P	Rated power	250kW	ω	Rated grid frequency	2π 50Hz
V_{dc}	Rated DC voltage	35kV	N	Module number / arm	15
C	Capacitance (std. operation [4])	$56\mu\text{F}$	v_{dc}^Σ	DC offset voltage (std. op. [4])	27.765kV
$v_{C,max}$	Maximum module voltage	2.2kV	i_{max}	Maximum arm current	34 A
L_g	Grid inductance	0mH	R_g	Grid resistance	0Ω
L_a	Arm inductance	26.8 mH	R_a	Arm resistance	0.1Ω

Table II: MMC PARAMETERS (HVDC CASE, based on [15])

Symbol		Value	Symbol		Value
V_g	Rated grid voltage	220kV	I_g	Rated grid current	4.454kA
P	Rated power	1200MW	ω	Rated grid frequency	2π 50Hz
V_{dc}	Rated DC voltage	400kV	N	Module number / arm	130
C	Capacitance (std. operation [4])	35 mF	v_{dc}^Σ	DC offset voltage (std. op. [4])	380.22kV
$v_{C,max}$	Maximum module voltage	3kV	i_{max}	Maximum arm current	5.7kA (+5 %)

To compare the results of [9, 10, 11] with those of the procedure presented in this paper, the first fitness function of the optimization scheme given in Sec. 3 is modified to represent the change in energy fluctuation $\Delta w_{1u}(\mathbf{x})/\Delta w_{1u}(\mathbf{x} = \mathbf{0})$. Note that $\Delta w_{1u}(\mathbf{x})$ is independent of w_{dc} , such that it is not necessary to find to minimum k_{dc} as done in (7) - (9) and the fitness function boils down to evaluating (5) and finding its maximum and minimum. With this change, the optimization is performed again and the resulting solutions are mapped on the originally proposed fitness function by applying (11). The resulting Pareto fronts are also plotted in Fig. 3 and 5 using dashed lines in the same colour coding as described before. Besides the overview in Fig. 3 and 5, the numerical values for the comparison are also given in Table III.

The presented optimization procedure outperforms all methods from literature in all cases. In the MV case, capacitance value savings of up to 35 % are possible without increasing the mean rectified arm current. However, this comes at the price of a comparably high CM voltage. If CM voltage injection must be avoided, the required capacitance value can be decreased by up to 26.6 % while the mean rectified arm current increases by 2.8 % only. When comparing to the methods that optimize the energy fluctuation only, the procedure proposed in this paper results in a 13.3 % smaller required capacitance value if CM voltage injection is allowed.

In the HVDC case, capacitance value savings of up to 82.7 % are possible without increasing the mean rectified arm current and with an increase in the maximum arm current of less than 5 %. The injected CM voltage is always less than the usual $\hat{v}_g/6$ in this case. If CM voltage injection must be avoided completely, the required capacitance value can be decreased by up to 51 % while the mean rectified arm current is still not increased. When comparing to the methods that optimize the energy fluctuation only, the procedure proposed in this paper results in a 42.5 % smaller required capacitance value if CM voltage injection is allowed.

5 Closed Loop Simulation

Generally speaking, any cascaded PI control system for MMCs can be adopted to successfully implement the harmonics injection presented in this paper. However, the controllers must be tuned for a comparably low bandwidth in order to not exceed the maximum allowed available arm voltage and to keep the available arm voltage high enough to avoid saturation. For better control performance, the control algorithms presented in [16, 17] can also be used.

The simulation results presented in Fig. 6 have been obtained with a slightly adopted version of the algorithm presented in [17]: The reference trajectories of the arm energies, the circulating currents and the controller output voltages are matched with the optimization results scaled by the reference power rated with the nominal power of the converter. This means that e.g. no CM voltage and no circulating current are injected at zero reference power. The simulation model is realized with an average arm model similar to the one proposed in [13]. Because of the voltage drop across the arm inductors which is not considered within the optimization procedure, the capacitance value obtained by the optimization procedure is increased by 5 % as well as the average arm voltage DC offset

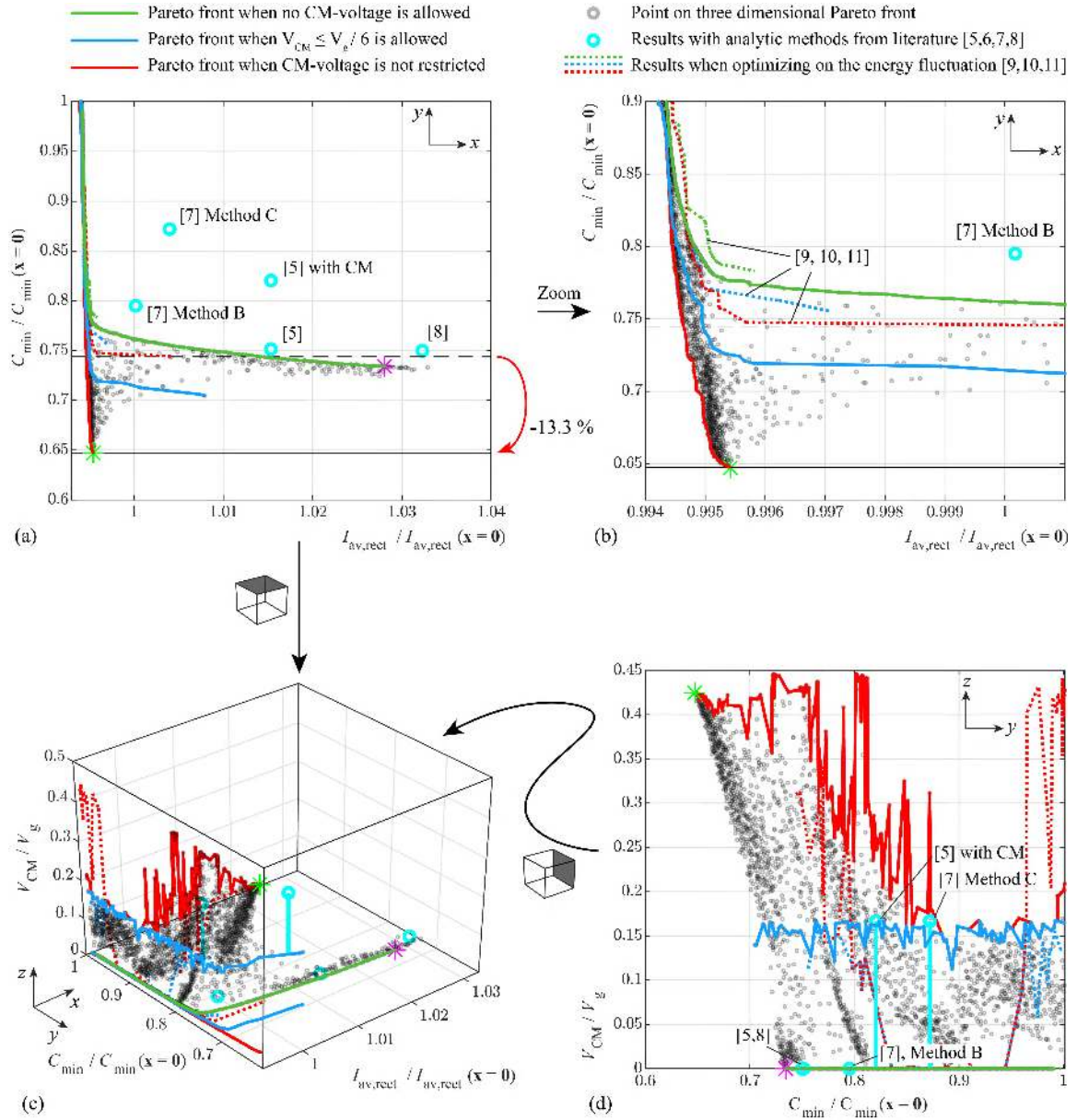


Fig. 3: Optimization results for the MV application MMC parameters in Tab. I. The dashed lines represent the results achieved with the methods from [9, 10, 11]. (a) Top view of c. Black horizontal lines show the difference in the minimum required capacitance value with the presented method vs. [9, 10, 11]. (b) Detail view of a. (c) Three dimensional Pareto front. (d) Side view of c.

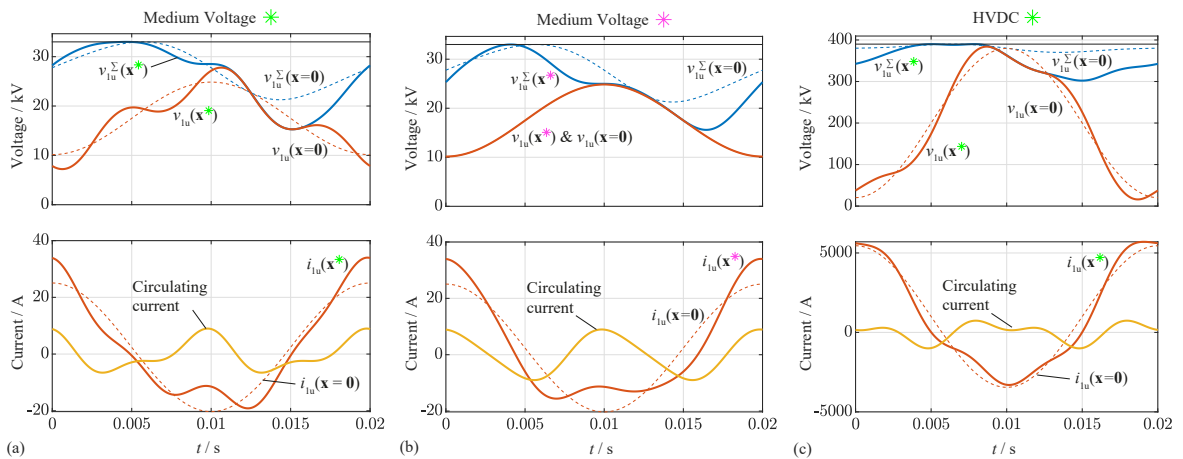


Fig. 4: Time domain trajectories for the points marked in Fig. 3 and 5. The dashed lines represent the trajectories with the minimum required capacitance value without any circulating current or CM voltage injection ($x=0$).

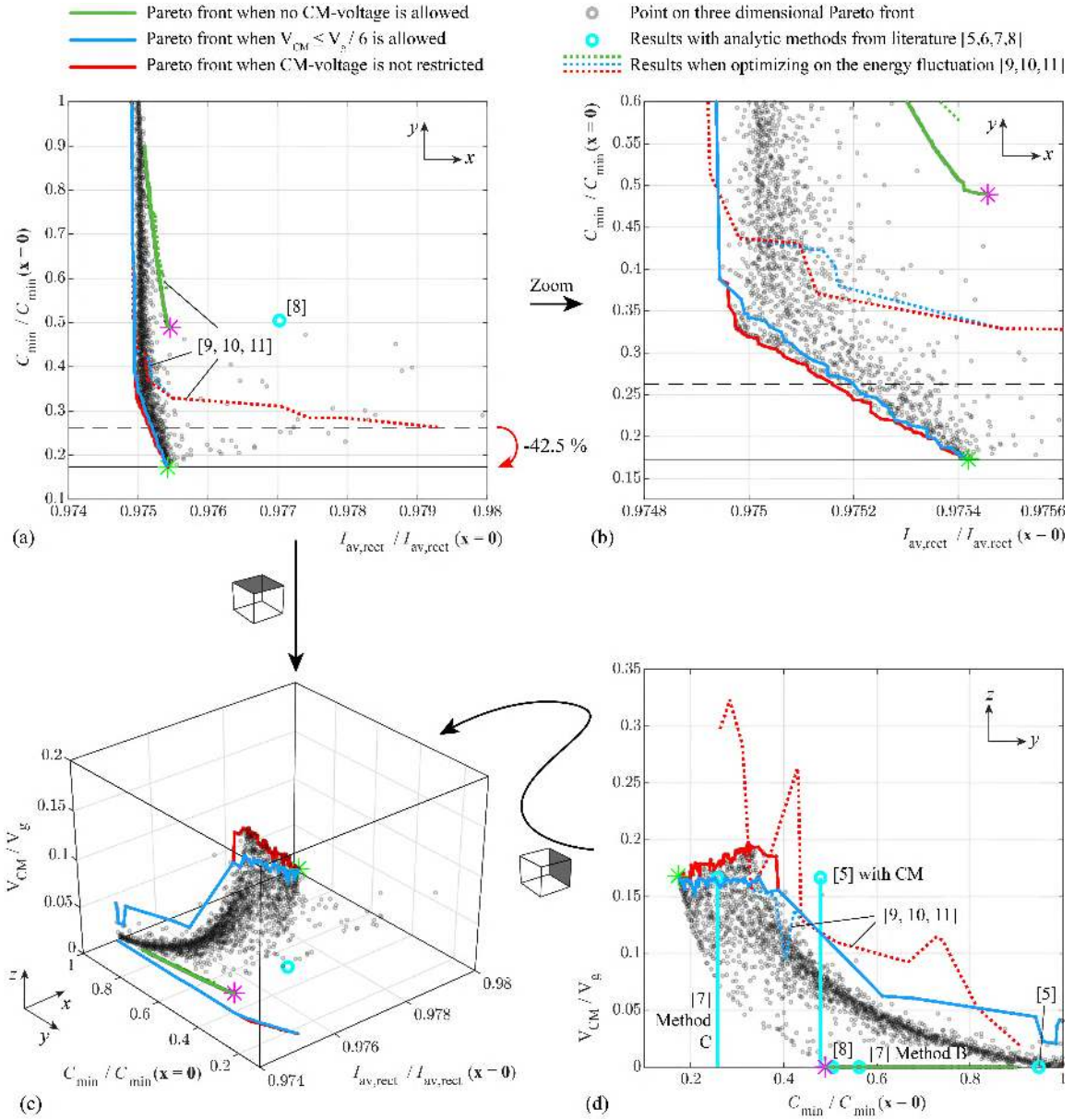


Fig. 5: Optimization results for the HVDC application MMC parameters in Tab. II. The dashed lines represent the results achieved with the methods from [9, 10, 11]. (a) Top view of c. Black horizontal lines show the difference in the minimum required capacitance value with the presented method vs. [9, 10, 11]. (b) Detail view of a. (c) Three dimensional Pareto front. (d) Side view of c.

Table III: COMPARISON WITH METHODS FROM LITERATURE

Reference	MV (Tab. I, Fig. 3)			HVDC (Tab. II, Fig. 5)		
	J_{cap}	$J_{current}$	J_{CM}	J_{cap}	$J_{current}$	J_{CM}
Point *	0.734	1.028	0	0.489	0.976	0
Point *	0.647	0.995	0.425	0.173	0.975	0.1684
[8]	0.750	1.032	0	0.505	0.977	0
[5]	0.751	1.015	0	0.948	1.053	0
[5] with CM	0.820	1.015	0.166	0.479	1.053	0.166
[7] method B	0.795	1.000	0	0.562	0.998	0
[7] method C	0.872	1.004	0.166	0.258	1.012	0.166
[9, 10, 11] without CM	0.783	0.996	0	0.576	0.975	0
[9, 10, 11] with CM	0.744	1.004	0.310	0.263	0.979	0.293

Table IV: CONTROLLER PARAMETERS

Parameter	Value	Parameter	Value
Sampling frequency	7.5 kHz	DC current weighting factor	100
Circ. current weighting factor	0	AC current weighting factor	0
Arm energy weighting factor	100	Control effort weighting factors (e)	1000
Control effort weighting factors (a)	10^5		

v_{dc}^{Σ} by 1%. Therefore, the arm voltage trajectories do not look exactly the same as in Fig. 4a. Due to the very low margin between the required and the available arm voltage, the power reference changes are implemented as ramp commands and not as step commands to avoid saturation effects. Moreover, the increase in the amplitude of the injected circulating currents and CM voltage during the increase of the power reference can be shown nicely during the power reference changes ($t = 10 \dots 50$ ms and $t = 150 \dots 240$ ms). All controller parameters are given in Tab. IV.

6 Conclusion

In this paper, an optimization scheme minimizing the energy storage requirements and therefore the necessary module capacitance value of MMCs is proposed. The scheme identifies the optimal combinations of an AC common mode voltage and a circulating current injection in order to shape the trajectories of the available arm voltages and the required arm output voltages such that the required capacitance value is minimized rather than the capacitor voltage fluctuation/ripple. The result of the optimization scheme is presented as a Pareto front to visualize the trade-off between required module capacitance value, semiconductor conduction losses, and the maximum injected AC common mode voltage.

For an exemplary MV MMC, a capacitance value reduction of almost 35% is achieved without increasing the mean rectified arm current compared to the standard operation without harmonics injection. Methods from literature achieve a reduction in the required capacitance value of only 25% compared to the standard operation. In case CM voltage injection is not allowed (e.g. due to a grounded star point at the AC side), the proposed optimization scheme achieves a reduction of the required capacitance value by up to 27%. Here, the increase of the mean rectified arm current is lower than 3%. For the considered HVDC application, a capacitance value reduction of almost 83% is achieved while the maximum arm current is constrained to be only 5% higher than in the standard operation without harmonics injection. The mean rectified arm current is not increased. State-of-the-art methods achieve a reduction in the required capacitance value of 52% only. Therefore, the capacitance value with the proposed optimization scheme is 42.5% lower compared to the state-of-the-art. Without CM voltage injection, the proposed optimization scheme decreases the required capacitance value by up to 51% without increasing the mean rectified arm current. Therefore, the presented optimal trajectory shaping scheme can be used to dramatically decrease the energy storage requirements of MMCs while keeping the conduction losses as low as possible.

Acknowledgements

This research is part of the activities of the Swiss Centre for Competence in Energy Research on the Future Swiss Electrical Infrastructure (SCCER-FURIES), which is financially supported by the Swiss Innovation Agency (Innosuisse - SCCER program).

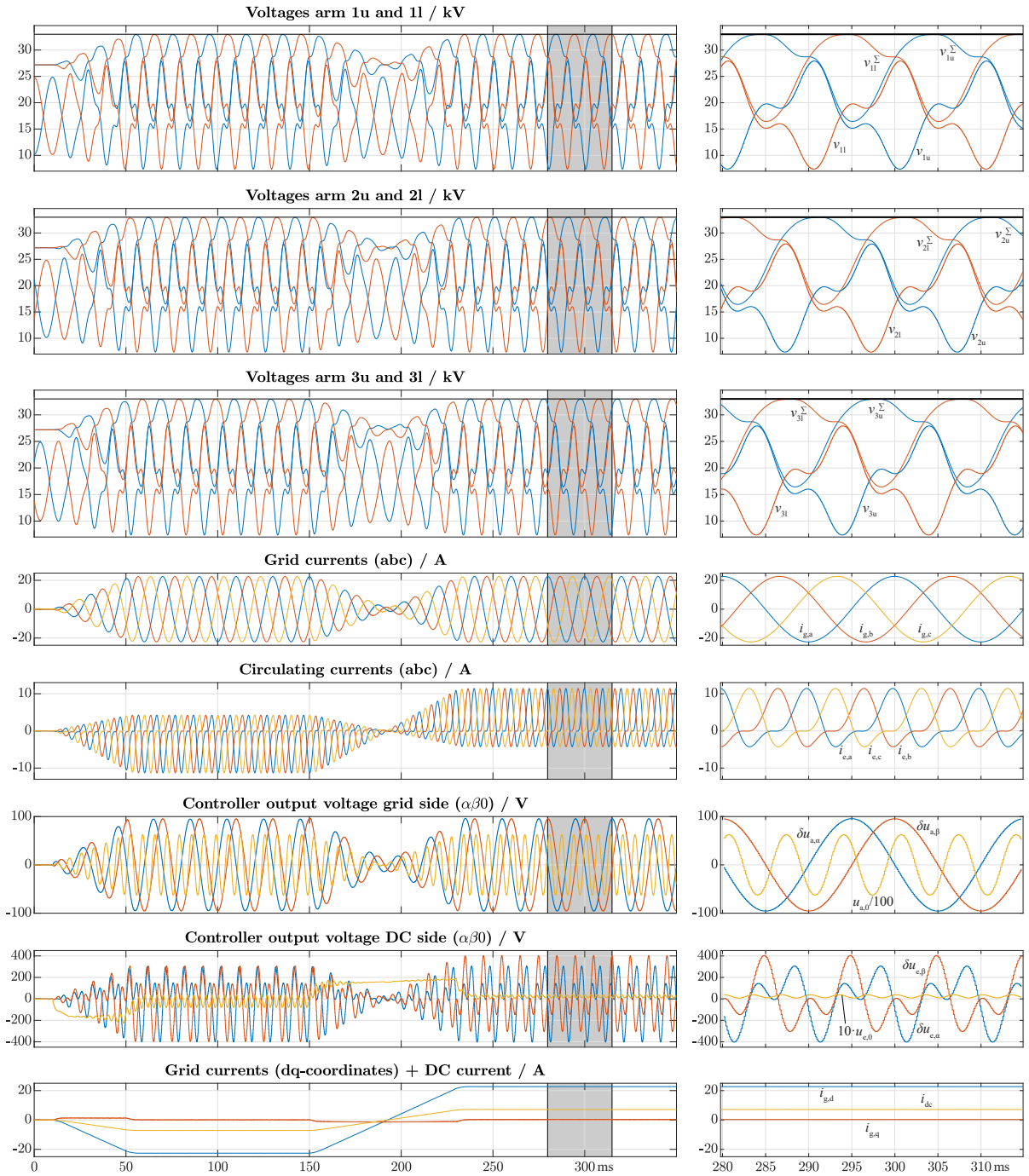


Fig. 6: Simulation results for the MMC design for the parameters given in Tab. I except for a reduced module capacitance value of $38 \mu\text{F}$ and the optimized trajectories marked with * in Fig. 3. A slightly adopted version of the controller presented in [17] is used. The controller parameters are given in Tab. IV. The left part presents an overview, while the right part represents a zoom-in of the time range marked in grey in the left part.

References

- [1] A. Lesnicar and R. Marquardt, "An innovative modular multilevel converter topology suitable for a wide power range," in *Power Tech Conf.*, vol. 3, 2003.
- [2] M. A. Perez, S. Bernet, J. Rodriguez, S. Kouro, and R. Lizana, "Circuit topologies, modeling, control schemes, and applications of modular multilevel converters," *IEEE Trans. on Power Electron.*, vol. 30, no. 1, Jan. 2015.
- [3] S. Debnath, J. Qin, B. Bahrani, M. Saedifard, and P. Barbosa, "Operation, Control and Appl. of the Modular Multilevel Converter: A Review," *IEEE Trans. on Power Electron.*, vol. 30, no. 1, 1 2015.
- [4] K. Ilves, S. Norrga, L. Harnfors, and H.-P. Nee, "On Energy Storage Requirements in Modular Multilevel Converters," *IEEE Trans. on Power Electron.*, vol. 29, no. 1, 2014.
- [5] J. Pou, S. Ceballos, G. Konstantinou, V. G. Agelidis, R. Picas, and J. Zaragoza, "Circulating current injection methods based on instantaneous information for the modular multilevel converter," *IEEE Trans. on Ind. Electron.*, vol. 62, no. 2, Feb 2015.
- [6] J. Wang, X. Han, H. Ma, and Z. Bai, "Analysis and injection control of circulating current for modular multilevel converters," *IEEE Trans. on Ind. Electron.*, vol. 66, no. 3, March 2019.
- [7] H. Fehr and A. Gensior, "Model-based circulating current references for mmc cell voltage ripple reduction and loss-equivalent arm current assessment," in *21st Europ. Conf. on Power Electron. and Appl. (EPE, ECCE Europe)*, 2019.
- [8] K. Ilves, A. Antonopoulos, L. Harnfors, S. Norrga, L. Ångquist, and H. Nee, "Capacitor voltage ripple shaping in modular multilevel converters allowing for operating region extension," in *37th An. Conf. of the IEEE Ind. Electron. Soc. (IECON)*, Nov 2011.
- [9] S. P. Engel and R. W. De Doncker, "Control of the Modular Multi-Level Converter for minimized cell capacitance," in *14th Europ. Conf. on Power Electron. and Appl. (EPE)*, 2011.
- [10] R. Picas, J. Pou, S. Ceballos, J. Zaragoza, G. Konstantinou, and V. G. Agelidis, "Optimal injection of harmonics in circulating currents of modular multilevel converters for capacitor voltage ripple minimization," in *IEEE ECCE Asia Downunder*, June 2013.
- [11] D. Townsend, G. Mirzaeva, and G. C. Goodwin, "Capacitance minimization in modular multilevel converters: A reliable and computationally efficient algorithm to identify optimal circulating currents and zero-sequence voltages," in *IEEE 12th Int. Conf. on Power Electron. and Drive Sys. (PEDS)*, Dec 2017.
- [12] J. A. Houldsworth and D. A. Grant, "The use of harmonic distortion to increase the output voltage of a three-phase pwm inverter," *IEEE Trans. on Ind. Appl.*, vol. IA-20, no. 5, Sep. 1984.
- [13] H. Bärnklaue, A. Gensior, and S. Bernet, "Derivation of an equivalent submodule per arm for modular multilevel converters," in *15th Int. Power Electron. and Motion Control Conf. (EPE/PEMC)*, 2012.
- [14] MathWorks. (2019) gamultiobj - find pareto front of multiple fitness functions using genetic algorithm. [Online]. Available: <https://www.mathworks.com/help/gads/gamultiobj.html>
- [15] CIGRE, "Guide for the development of models for HVDC converters in a HVDC grid," 2014.
- [16] S. Fuchs, M. Jeong, and J. Biela, "Long horizon, quadratic programming based model predictive control (MPC) for grid connected modular multilevel converters (MMC)," in *45th Ann. Conf. of the IEEE Ind. Electron. Soc. (IECON)*, Oct 2019.
- [17] M. Jeong, S. Fuchs, and J. Biela, "High performance LQR control of modular multilevel converters with simple control structure and implementation," in *22nd Europ. Conf. on Power Electron. and Appl. (EPE'20, ECCE Europe)*, Sept 2020.